Picosecond photofragment spectroscopy. IV. Dynamics of consecutive bond breakage in the reaction C2F4I2→C2F4+2I

Lutfur R. Khundkar and Ahmed H. Zewail

Citation: The Journal of Chemical Physics **92**, 231 (1990); doi: 10.1063/1.458469
View online: http://dx.doi.org/10.1063/1.458469
View Table of Contents: http://scitation.aip.org/content/aip/journal/jcp/92/1?ver=pdfcov
Published by the AIP Publishing

Picosecond photofragment spectroscopy. IV. Dynamics of consecutive bond breakage in the reaction $C_2F_4I_2 \rightarrow C_2F_4 + 2I$

Lutfur R. Khundkar[a] and Ahmed H. Zewail
Arthur Amos Noyes Laboratory of Chemical Physics,[b] *California Institute of Technology, Pasadena, California 91124*

(Received 12 May 1989; accepted 25 September 1989)

Picosecond photofragment spectroscopy of the ultraviolet (UV) photodissociation of 1,2-diiodotetrafluoroethane reveals consecutive breaking of the two C–I bonds. Spin–orbit excited (I*) atoms show a prompt rise, in agreement with a direct mode dissociation of the first bond. Ground-state (I) atoms show a biexponential buildup, one component being fast ($\leqslant 1$ ps) while the other component is slow (30–150 ps depending on total energy), characteristic of the second bond breaking. The transient behavior of I atoms changes with the available energy. These results are interpreted in terms of a two step model involving a weakly bound radical. Simulations of transient behavior of I atoms, based on estimated internal energy distributions from the primary step and a model for dissociation rates as a function of energy, suggest that surface crossings are relevant to the dynamics and that the quantum yield of I atoms varies with excitation energy.

I. INTRODUCTION

In previous publications from this laboratory,[1] we have reported on studies of state-to-state reaction dynamics using picosecond photofragment spectroscopy. The reactions studied involve a "simple" bond breaking process, e.g., $NCNO \rightarrow CN + NO$, $HOOH \rightarrow OH + OH$, and $CH_2{=}C{=}O \rightarrow CH_2 + CO$. Here, we are concerned with reactions of molecules with two identical bonds (ICF_2CF_2I) where, in principle, both *consecutive* and *concerted* bond fission are possible. For 1,2-diiodotetrafluoroethane, our preliminary time-resolved data[2] indicated that there are two consecutive steps with drastically different time scales for the primary and secondary dissociation:

$$C_2F_4I_2 \rightarrow C_2F_4I\cdot + I$$

$$C_2F_4I\cdot \rightarrow C_2F_4 + I.$$

The first step is characteristic of alkyl halide[3,4] bond breaking, with dissociation times being $\leqslant 1$ ps, as determined by Knee *et al.*[2]

The photodissociation of alkyl halides by ultraviolet (UV) radiation in the 200–300 nm range has been studied extensively.[5] In the case of the iodide, the excitation involves the promotion of a nonbonding electron from the iodine $5p\pi$ atomic orbital to a σ^* molecular orbital. The absorption is broad and the upper state is believed to be repulsive. Photofragment angular distribution measurements suggest that the dissociation is one of the direct mode type. Many of the polyhaloalkanes show absorption spectra that appear to be superpositions of the individual monohaloalkanes. This suggests that the different chromophores are only weakly coupled and therefore bond-selective dissociation may be possible. Such experiments have met with some success. Lee and co-workers have shown that photodissociation of C_2F_4IBr at 193 nm[6] yields I atoms in the first step, even though the photoexcitation involves a Br electron. They also found that in the case of CH_2IBr,[7] I or Br are produced almost exclusively, depending on the excitation wavelength.

Since the two C–I chromophores of $C_2F_4I_2$ are identical by symmetry, the absorption process cannot distinguish between them. However, we have previously reported different dissociation rates of $C_2F_4I_2$ into the two accessible states of the I atom, $I^*(^2P_{1/2})$ and $I(^2P_{3/2})$ (see Fig. 1).[2] Signal from $I^*(^2P_{1/2})$ atoms showed a fast ($\leqslant 1$ ps) rise, corresponding to the prompt breakage of the first C–I bond. The population of ground-state iodine atoms was observed to accumulate with an apparent biexponential form, the slow component (~ 30 ps) corresponding to the secondary fragmentation process. This paper represents a more complete study of the dissociation processes occurring in this molecule. The results are analyzed in terms of a two-step mechanism, involving a short-lived intermediate—the C_2F_4I radical. The first step is a direct dissociation, while the second one is the complex mode unimolecular dissociation of internally excited C_2F_4I. Our previous finding[2] and the conclusions of the present paper are in agreement with recent measurements of velocity and angular distributions of the products of photodissociation.[8,9]

To characterize the dynamics and deduce the mechanism of the reaction, we present details of the energy dependence of the rates in both accessible product channels. The dependence of the long component of I atom buildup on the excitation energy follows our intuition: lower total energy leads to lower internal energy in the intermediate radical, which therefore decays more slowly. The commonly used impulsive models[10] for predicting energy distributions of a direct mode reaction are applied to estimate the internal energy in the radical following the initial dissociation, which is then used to estimate rates. Simulations of the temporal behavior of I atoms using these rates and crude energy distribution functions are compared with the experimental tran-

[a] Present address: Jet Propulsion Laboratory 67-201, C.I.T., Pasadena, California 91109.
[b] Contribution No. 7949.

 0021-9606/90/010231-12$03.00

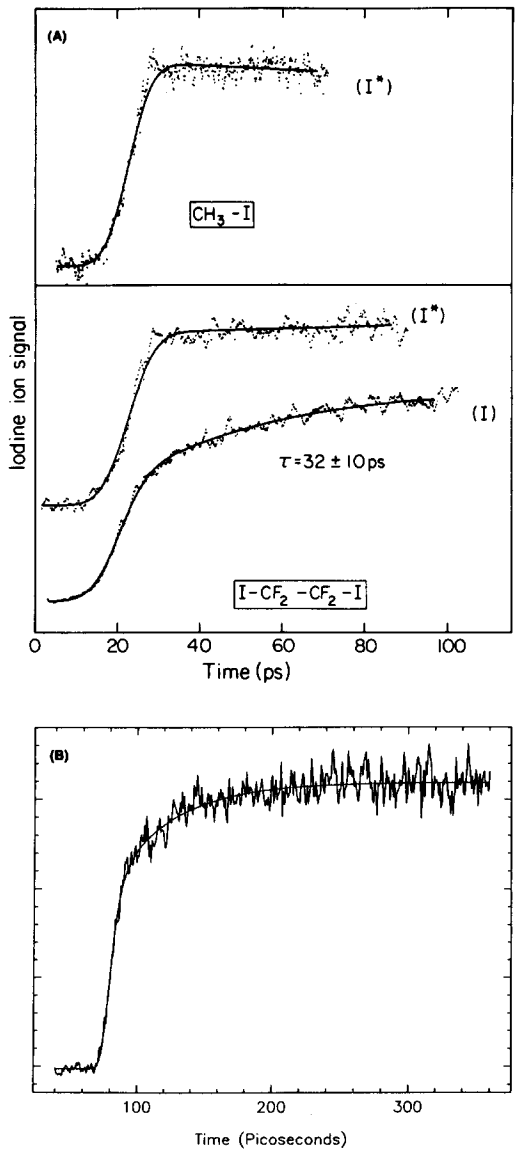

FIG. 1. Transient behavior of I and I* channels. (a) is the same as in Ref. 2, indicating the similar dissociation rates in the I* channel and in methyl iodide. The nonexponential buildup in the I channel is evident. (b) shows the behavior in that channel over a longer time range, thus emphasizing the slow component(s).

sients in an attempt to show that the observed biexponential behavior is consistent with a wavelength-dependent quantum yield of I atoms in the primary dissociation.

The body of the paper is structured as follows. Experimental details are presented in Sec. II. The results are presented along with their interpretation in Sec. III which is divided into three main parts. Section III A consists of a brief review of the states involved in the excitation. A simple exciton model is applied to $C_2F_4I_2$ and the effects of the dipolar coupling on dissociation are considered in this subsection. Section III B discusses the transient behavior of the spin–orbit excited I atom while Sec. III C contains a detailed discussion of the transient behavior of ground-state I atoms as a function of the excitation energy. Various explanations for a nonexponential buildup are considered. The pump and probe power dependences are used to assess the involvement of multiple-photon dissociative pathways (Sec. III C 1). The effects of a distribution of internal energies on the dynamics are considered in Secs. III C 2 and III C 3. In the former part, we review the models used for estimating energy distributions and rates. Details of numerical simulations assuming unit quantum yield of I* atoms in the first step are presented. In Sec. III C 3, we discuss the possibility of energy-dependent quantum yields of I atoms in the primary dissociation and present a second set of simulations. A general evaluation of the results of these simulations (Sec. III C 4) precede the conclusions from this study.

II. EXPERIMENTAL

Details of the experimental apparatus have been presented elsewhere[1,11] and we provide only a brief description here. The output of a mode-locked CW YAG laser was frequency doubled and used as the source for two independently tunable, synchronously pumped dye lasers (R6G). The tuning element in each case was an intracavity quartz birefringent filter. The output of each laser was amplified and frequency doubled to obtain the desired pump and probe frequencies. Cross correlations of the visible output were typically Gaussian, with ~8–10 ps full-width at e^{-1} of the maximum.

The two amplified beams were passed along different arms of a Michelson interferometer, recombined on a dichroic mirror and propagated collinearly from there on. Since both the pump and probe wavelengths were in the ultraviolet (UV) range of the spectrum, the visible beams had to be frequency doubled. Efficient recombination of the beams was achieved by using a nonlinear crystal in one arm of the interferometer and using a dichroic mirror that reflects UV and transmits visible wavelengths as the recombiner. The second visible beam was frequency doubled after the two beams had been recombined. The two UV beams were then focused in the ionization region of a time-of-flight mass spectrometer (TOFMS) mounted on a molecular beam apparatus with a 25 cm focal length lens made of fused silica. One of the arms of the interferometer had a nominal $\times 1$ telescope that was adjusted to compensate for the slight difference in the focal length of the two colors, thereby improving the efficiency of probing the species created by the pump laser beam. A polarization rotator and a polarizer were installed in each arm of the interferometer to permit fine control of the intensity in each beam.

1,2-diiodotetrafluoroethane ($C_2F_4I_2$) was obtained from Specialty Chemicals ($\geqslant$97% purity) and used without further purification in the experiments described below. The sample was kept in a stainless-steel bomb maintained at 0 °C. Helium gas at a pressure of 20 psig was flowed over the sample and expanded through a pulsed nozzle (Kel-F) with a 500 μm aperture. The expansion was skimmed ~1 cm from the valve and the total distance from the nozzle to the ionization region was ~10 cm. Mass spectra obtained using laser multiphoton ionization (MPI) showed no evidence of clusters. The signal was averaged in a boxcar with the gate set to sample only the portion of the detector output which

corresponded to species having the same mass-to-charge ratio as I^+.

The sample had a slight violet coloration due to the presence of molecular iodine which is produced when $C_2F_4I_2$ decomposes. The following tests were performed to estimate the contribution of contaminants to the signal. First, we considered the possibility of I_2 as a contaminant. It is known[5] that I_2 absorption at the pump wavelengths is weak. We performed the experiments with sample that had been treated with metallic copper (I_2 scavenger) and used a glass trap with teflon stopcocks and lines to minimize decomposition catalyzed by metal surfaces. The results were identical to those obtained with the sample in the steel bomb, implying that the observed signal had no significant contribution from I_2. Second, transients measured with the sample at room temperature (higher vapor pressure) were not significantly different from those measured with the sample cooled to 0 °C. This emphasizes the absence of I_2 as a contaminant and indicates that clusters of $C_2F_4I_2$ do not contribute to the signal. Finally, ^{19}F NMR of the sample showed a single peak in greater than 99% abundance which was assigned to $C_2F_4I_2$ by comparison with published NMR data.[12] The absence of other significant peaks in the spectrum show that no other fluorinated species were present in the sample. We therefore concluded that the signal measured was from I–CF_2CF_2–I alone.

The probe laser (DL1) was tuned to a two-photon transition[13] in neutral atomic iodine. The transition could be chosen to originate from either the ground state ($^2P_{3/2}$) or the excited spin–orbit state ($^2P_{1/2}$) using light at 3047 or 3040 Å, respectively, thus offering a means of distinguishing the two channels. The resonance enhancement with the probe alone was greater than one order of magnitude, providing excellent selectivity for probing atomic iodine. The pump laser (DL2) was tuned to frequencies convenient for amplification. Transients were recorded over a range of pump wavelengths from 279 to 307 nm.

The rotator–polarizer combination was particularly useful in measuring the intensity dependence of each laser. The output of the boxcar averager was sampled with a microprocessor controlled 12 bit analog-to-digital converter. This allowed the determination of average values and standard deviations (quoted errors) for a given level of pump and probe intensity. The background was carefully accounted for by measurements of the signal with each laser alone.

The deduction of characteristic constants (lifetimes) from the raw data requires knowing the proper instrument response function. The correct system response function for these experiments is a difficult entity to measure experimentally. A truly instantaneous process which involves the same orders of nonlinearity for the pump and probe as in these experiments is required. A process which is known to occur in less than 100 fs may be used as an approximation. A likely candidate would be the dissociation of methyliodide, believed to be ~70 fs. Another candidate is dissociation of $C_2F_4I_2$ into the I* channel. The first involves the risk of contamination of the beam, and the rate of the latter is an unknown quantity. It also involves tuning DL1, which introduces a possible source of error. For the majority of the fits reported here, we assumed that the system response function was Gaussian and attempted to fit the initial rise by varying the width of the response. The typical width determined this way was ~8 ps. This is shorter than the visible cross correlations, most likely because the signal depends nonlinearly on the intensities of both visible beams.

Characteristic time constants and relative amplitudes for the results obtained using an on-resonance probe were deduced using a nonlinear least squares optimization routine.[14] Each transient was fitted multiple times to avoid bias from the choice of initial parameters for the algorithm. Many transients recorded at the same pump and probe wavelengths were analyzed to determine the accuracy of the results reported here. The transients presented in the figures below were all smoothed using a three-point averaging algorithm. In each case, the *raw* data were analyzed and the best fit line (in the least-squares sense) was similarly smoothed and superimposed on the data. Thus numerical averaging had no effect on the derived rate constants.

III. RESULTS AND DISCUSSION

In the present study, we have measured the buildup of iodine atoms in both ground and spin–orbit excited state at several different pump wavelengths in the range 279 to 307 nm. Figure 1 shows typical results for the buildup of population in these two channels. The basic findings are that I* atoms are produced essentially instantaneously ($\leqslant$1 ps), whereas I atoms are produced with an apparent time-dependent rate constant (i.e., the observed behavior is nonexponential). This complex temporal behavior can be modeled as a two-component exponential buildup. The photolysis wavelength has no apparent effect on the rate of production of I* atoms but can significantly alter the rate of formation of I atoms. Transients obtained while monitoring the latter channel for different photolysis wavelengths are shown in Fig. 2. They show a trend toward longer lifetimes (~30 to ~150 ps) with lower excitation energy and a concomitant increase in the fraction of the fast component.

These results can be described in terms of a two-step, sequential bond fission process

$$C_2F_4I_2 \rightarrow C_2F_4I^\dagger + I^{(1)}, \quad (1)$$

$$C_2F_4I^\dagger \rightarrow C_2F_4 + I^{(2)}. \quad (2)$$

Superscripts on the I atom differentiate between the products of each step. The first step is expected to be impulsive, i.e., fast. The radical C_2F_4I is formed with a distribution of internal energies and can undergo subsequent dissociation with a range of rate constants. Excitation at different pump frequencies should affect the energy content of the nascent radical and hence its rate of decomposition. These observations appear to be qualitatively consistent with the experimental results. A quantitative comparison with the predictions of models for radical decomposition is attempted below. We place special emphasis on the different processes which may contribute to the observed nonexponential buildup in the I channel.

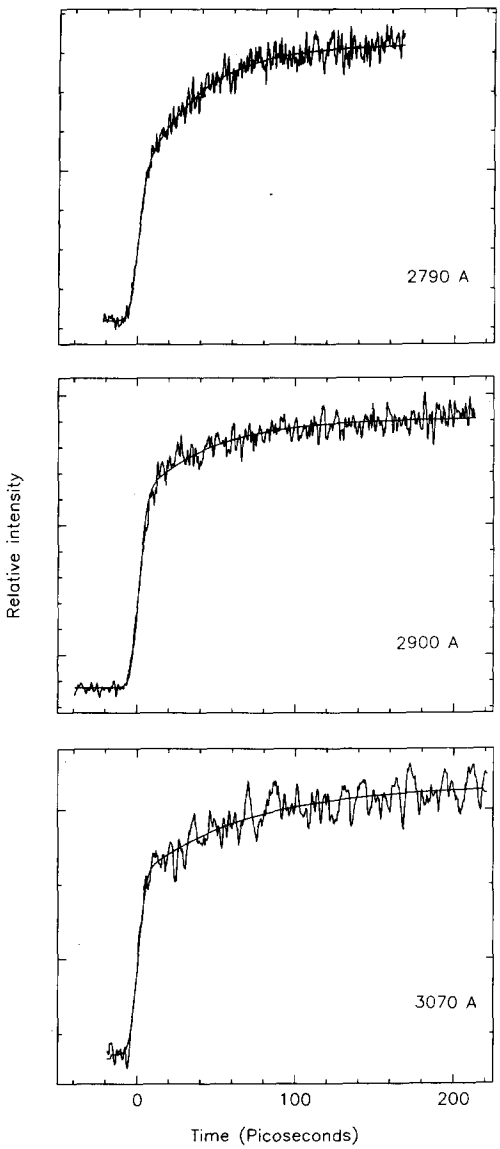

FIG. 2. Transient buildup of I atoms as a function of the pump wavelength. (a) 278.6 nm; (b) 290 nm and (c) 307 nm. The solid line in each plot represents the fitted biexponential rise convoluted with an assumed Gaussian instrument response. Results of the fits are given in Table II.

A. Electronic states and the exciton model

A brief review of the states involved in the excitation process is pertinent. The A continuum in alkylmonoiodides is a spin-forbidden $n \rightarrow \sigma^*$ transition. The analysis for methyl iodide reveals five underlying states, three of which are symmetry allowed. According to the analysis of Mulliken,[5,15] one of these states ($^3Q_0$, transition moment parallel to the C–I bond) correlates to I* products, while the other two (^1Q and $^3Q_1$, transition moments perpendicular to the C–I bond) correlate to ground state I. In most iodoalkanes, the state carrying the oscillator strength correlates to excited iodine atoms. Ground state atoms are presumably formed via a surface crossing. Fluorine substitution on these alkanes reduces the strength of the coupling between the excited states. This often results in high quantum yields in the I* channel,[16] as has been demonstrated for compounds such as CF_3I and C_2F_4IBr which have I* quantum yields of almost unity at 266 nm. By analogy, we expect that the same is true for our sample.

$C_2F_4I_2$ is a symmetric molecule with two chromophores and one must consider the effects of any interaction between them on the dynamics of dissociation. The chromophores are exactly degenerate to zero order. Since the point group of $C_2F_4I_2$ in its staggered or *anti* conformation (C_{2h}) does not have degenerate representations, they must interact with each other, at least to the extent of removing the strict degeneracy. A simple dipole–dipole interaction between the two halves would give rise to exciton states, which are the molecular eigenstates of the system if the coupling with the dissociative continuum is ignored. The absorption spectra of diiodomethane and iodoform have been described in terms of such a model.[17] Simple vector algebra may be used to determine the directions of the transition moments of the optically allowed exciton states. It is possible to show that only the *anti* conformer, where the carbon and iodine atoms are coplanar and arranged in a *trans* configuration, can give rise to values of the anisotropy parameter β close to 2.0. Since the measured β is 1.8, we conclude that the predominant conformer in the expansion is *anti*, the thermodynamically favored form.

The absorption maximum for $C_2F_4I_2$ vapor is at 266 nm,[18] essentially the same as for CF_3I, suggesting that the interaction between the two chromophores is weak and obscured by the width of the absorption band. The strength of this coupling is to be compared with the coupling of the zero-order molecular state to the dissociation continuum. If dissociation occurs much faster than the rate of dephasing of the initial state, then the description in terms of local bond excitations is good. We then expect that each of the two chromophores should behave as the corresponding monochromophoric molecule, in this case CF_3I, to a first approximation. The quantum yield in the I* channel from the first step [Eq. (1)] should then be unity. The measured quantum yield at 266 nm ($\geqslant 0.95$) is consistent with this argument.

It is relevant to consider the effect of the excitonic interaction on surface crossings involving states of a given chromophore. One can show that the magnitude of the dipolar coupling does not affect the strength of the electronic coupling between different, monomer states if the cross-coupling terms can be neglected. On the other hand, if there is some interaction between two monomer states, one combination of exciton states will have increased mixing; the other three do not interact to first order. The energy at which these exciton components intersect may be somewhat different from that corresponding to the isolated chromophore. Consequently, the probability of state crossing at a given excitation energy, and therefore the quantum yield of I* in the primary step, may be different in the photolysis of $C_2F_4I_2$ than in CF_3I.

B. Dissociation into the I* channel

Product translational energy distributions from the dissociation of $C_2F_4I_2$ using 266 nm light measured by Reid *et al.*[8] show a sharp peak centered roughly at the same value of absolute translational velocity as observed in a similar study of C_2F_4IBr.[6] A second, broad peak has been ascribed to I

atoms from secondary dissociation. It is important to note that no additional peaks at higher translational energies were observed in this study, in contrast to the measurements on $C_2F_2H_2IBr$, where multiple pathways for primary dissociation are accessible. This constitutes strong evidence that in the dissociation of $C_2F_4I_2$ with 266 nm light, the initial step leads primarily to I* atoms.

Extrapolation of these results to lower excitation energies is made complicated by the results on the quantum yield of I* from $C_2F_4I_2$. A study of the IR fluorescence[18] using *n*-C_3F_7I as a standard concluded that the yield of I*was 0.9 at 308 nm. However, kinetic spectroscopy[9] of $C_2F_4I_2$ shows a much lower quantum yield for excited I atoms (0.6), which is outside the reported range of experimental error of Ref. 18. In our discussion below, we will consider both alternatives.

The direct dissociation step is expected to be fast, on the order of a vibrational period. Our observations of a prompt rise of population in both the ground and the excited spin–orbit state corroborate this directly. These measurements alone cannot determine the fraction of the ground state I atoms formed in the initial step for reasons discussed below. We may argue that only an insignificant amount of I* is produced in the secondary reaction in the following manner. Suppose some I is formed in the first step, which is fast. This would result in an additional 21.7 kcal/mol that must be dispensed between translation and internal degrees of freedom. If most of this energy appeared as internal energy, I* atoms could be formed in the second step. The energy available for this mode of breakup would be close to the threshold, and we would expect to observe a slow component in the rise of signal in the I* channel, similar to that seen in the buildup of the I atoms. Since we cannot discern a slow component in our measured transients, we conclude that at all wavelengths studied (279 to 307 nm), I* is formed only in the primary step.

C. Dissociation into the $I(^2P_{3/2})$ channel

As mentioned earlier, the dynamics of formation of ground state I atoms is complex and we consider several possible explanations in detail. Recently revised thermodynamic estimates indicate that the nascent radical C_2F_4I is weakly bound ($\sim$8 kcal/mol),[9] consistent with our previous report.[2] In principle, I atoms can be formed in both steps, provided that the fraction of total energy available as internal energy in the radical does not decrease drastically when the excitation energy is reduced. The secondary fragmentation process must lead to $I(^2P_{3/2})$ atoms exclusively if only I* atoms are formed in the first step, based simply on energy conservation. The rate equations appropriate for the proposed mechanism [Eqs. (1) and (2)] are readily solved. Assuming that the system starts with population only in $C_2F_4I_2$ {i.e., $N=[C_2F_4I_2](0)$} and the rates for the two steps are not equal, we obtain

$$[C_2F_4I_2](t) = Ne^{-k_1t}, \tag{3}$$

$$[C_2F_4I](t) = \frac{Nk_1}{k_1-k_2}(e^{-k_2t}-e^{-k_1t}), \tag{4a}$$

$$[I^{(1)}](t) = \frac{N}{k_1}(1-e^{-k_1t}), \tag{4b}$$

$$[C_2F_4](t) = [I^{(2)}](t) = \frac{Nk_1}{k_1-k_2}\left[(1-e^{-k_2t}) - \frac{k_2}{k_1}(1-e^{k_1t})\right]. \tag{5}$$

Equation (5) shows that the buildup of products of the secondary fragmentation may appear biexponential, with the relative amplitudes being inversely proportional to the rate constants, k_1 and k_2. In our results for I, $k_1 \geqslant 10^{12}$ s^{-1} and $k_2 \leqslant \frac{1}{30}k_1$, whereas the observed amplitudes of the two components are approximately equal in magnitude. It should be noted that convolution with a finite response function will not affect the relative amplitudes of the two components since we detect mostly long-lived species (stable products). Therefore, Eq. (5) does not correctly represent the dynamics observed in I channel and we must consider other proceseses which can result in a nonexponential buildup in this channel. Processes such as multiphoton absorption or direct dissociation into the I channel will affect the observed ratio of amplitudes. In addition, a distribution of values of k_2 will also affect the relative amounts of fast and slow components. We discuss these schemes in the following sections. Numerical simulations of the buildup of I atoms may provide an independent verification of the branching ratio in the initial step.

1. Sequential multiphoton absorption

Unstable radicals such as CH_2I[19] and $C_2F_2H_2Br$[9] have been shown to absorb 266 nm radiation. The cross section is generally comparable to that of the corresponding fully-saturated alkane having a single C–I or C–Br bond. Weakly bound radicals which absorb a second photon are highly internally excited and liable to dissociate very rapidly. This would open additional channels that must be considered in any description of the dynamics. The kinetic scheme shown in Fig. 3 shows all pathways that may lead to ground state I atoms. Since the detected signal is resonantly enhanced, we neglect pathways that lead to I^+ by direct absorption of more than one photon from the pump laser.[20]

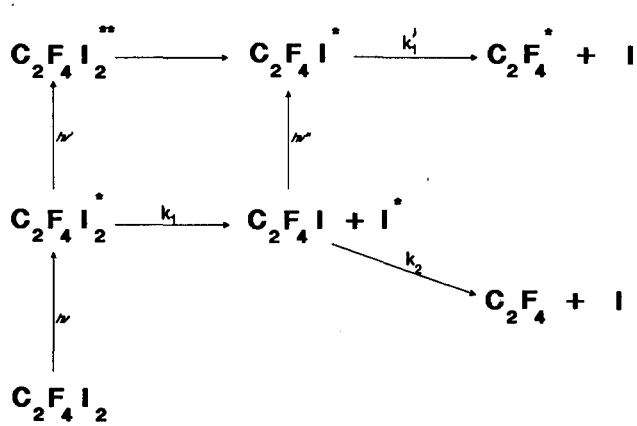

FIG. 3. Kinetic scheme for dissociation of neutral $C_2F_4I_2$ including pathways for multiphoton dissociation. The shaded arrows indicate optical transitions.

An approximate treatment of the effect of absorption of photons by any of the dissociating species on the subsequent evolution may be done in the following way: If either $C_2F_4I_2$ or C_2F_4I absorbs a pump photon, we may assume that the initial conditions are different. If we use the standard (Einstein) kinetic model for absorption of light, we can show that the correction involves adding a term

$$N'\alpha(1-e^{-k_1't})$$

to Eq. (5). If the parent molecule absorbs the photon, $N'=N$, whereas if it is absorbed by the radical, $N'=N(k_1\sigma/k_1-k_2)\alpha(1-e^{-k_1't})$, where N is the total number of absorbers in the excitation volume. Here, α is the product of the absorption cross section and the average intensity and σ is a function of the two rate constants, less than unity in magnitude. If k_1 is fast compared to the pulse duration and k_2 is slow, $\sigma\sim 1$. k_1' is an approximate rate constant for the appearance of iodine atoms from the more highly excited species ($C_2F_4I_2^{**}$ and $C_2F_4I^*$) shown in Fig. 3. Similarly, if either of these species absorbs a probe photon, the observed signal is the sum of Eq. (5) and a fraction, α' of either Eq. (3) or Eq. (4a). Assuming there is no significant difference in the absorption coefficient at the two different colors (pump and probe), α and α' are of the same order of magnitude. In either case, we see that the relative fraction of fast to slow changes by a number ($\sim\alpha$) which is generally small compared to unity. Transients obtained with pump pulses of different intensities are shown in Fig. 4. The fraction of fast component is clearly higher when the intensity is high. This is in qualitative agreement with this discussion. The amount of change is rather high ($\sim$20%), suggesting that the absorption cross section for the radical may be large.

Figure 5(a) shows a log–log plot of signal vs pump power while a similar plot of the probe power dependence appears in Fig. 5(b). These measurements show a linear dependence on the pump and a cubic dependence on the probe at low intensities. At higher pump intensities (not shown), one can see deviations from these simple power laws. This behavior suggests that other channels for dissociation may be accessible at such intensities. Since the transients measured with low pump and probe intensities clearly show the biexponential behavior, we conclude that our observations reflect an intrinsic property of the molecular species under study. Bearing in mind that sequential multiphoton absorption may distort experimental results, we collected most of our data under low pump and probe intensity (and hence low signal) conditions.

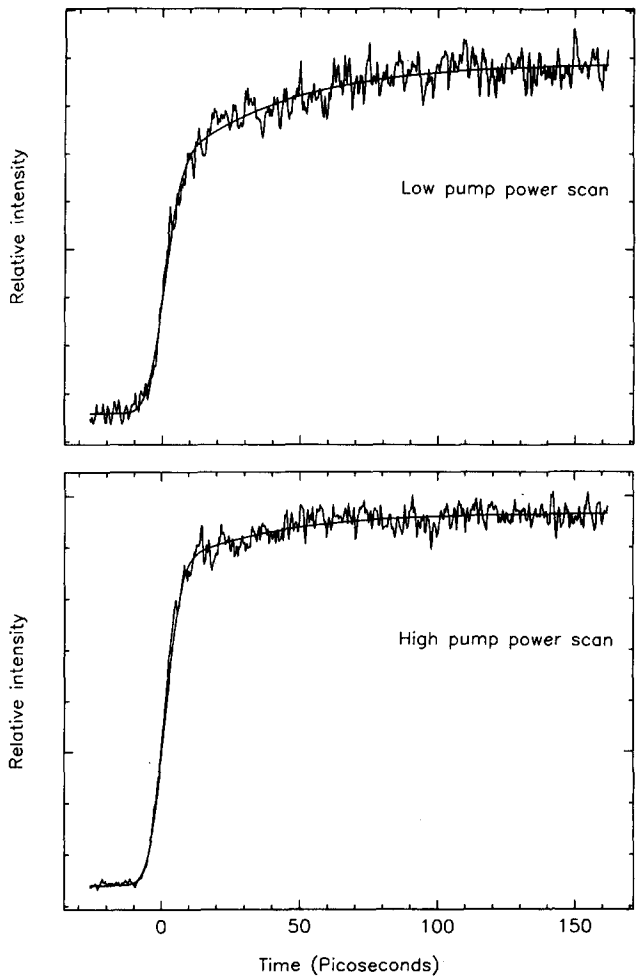

FIG. 4. Transients obtained with (a) weak and (b) intense pump pulses. The relative amplitude of the fast component is significantly higher in (b) than in (a).

2. Excitation energy and radical internal energy distribution

Kinetic spectroscopy shows a distribution of relative translational energies from the fragmentation process. The two step mechanism then implies that radicals are formed with a distribution of internal energies, complementary to the spread in translational energy of the I* atom and satisfying energy conservation. A recent estimate of the stability of C_2F_4I indicates that the radical is bound by 8.1 ± 1.5 kcal/mol ($2830\ cm^{-1}$).[9] Since the radicals are formed in a collisionless environment, no energy transfer between molecules can occur and they dissociate with individual rate constants, $k_2(E)$, which depend on the internal energy E. The corresponding distribution of lifetimes results in a nonexponential decay of the radicals which is often characterized as apparent biexponential behavior. The signal is the sum of exponential transients, each described by Eq. (5) and weighted by the probability density. In the limit of a continuous distribution of internal energies, the sum may be represented by an integral

$$S(t)=\int_{E_0}^{\infty}\frac{P(E)}{1-\zeta(E)}\Big[\Big(1-e^{-k_2(E)t}\Big)-\zeta(E)(1-e^{-k_1't})\Big]dE, \tag{6}$$

$$\approx\int_{E_0}^{\infty}\Big[1-e^{-k_2(E)t}\Big]P(E)dE \quad \text{if } \zeta(E)\ll 1, \tag{7}$$

where $\zeta(E)=k_2(E)/k_1$ and $P(E)dE$ is the probability that the radicals have energy in the range $(E,E+dE)$. E_0, the threshold for radical dissociation, is contained implicitly in the energy dependence of k_2. In our previous report[2] we

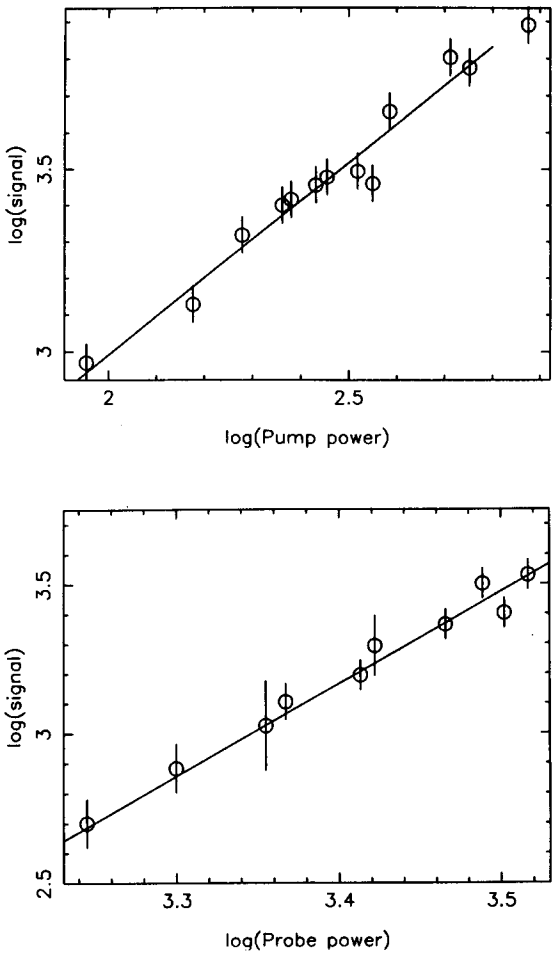

FIG. 5. (a) Dependence of the signal on the pump intensity. The slope of the best fit line shown is 1.1. (b) Probe-power dependence. The slope of the best fit line shown is 3.1.

showed that with a judicious choice of $k_2(E)$, the expression for the signal in Eq. (7), $S(t)$, convoluted with an instrument response function, could explain our observation of a biexponential buildup.

In order to develop a model of the dissociation processes which is consistent with our results at different excitation energies, we need to know: (i) the distribution of internal energy in the radicals at each excitation energy and the relative amounts of vibrational vs rotational excitation; (ii) the unimolecular rates, $k_2(E)$, as a function of energy and angular momentum; and (iii) the rate of formation of C_2F_4I, k_1. We discuss methods for estimating each of these unknowns in the next few sections.

a. Impulsive models for energy partitioning

A classical mechanical model[10,21] for predicting the average kinetic energy released in a direct dissociation has been proposed and applied to the UV fragmentation of many alkyl halides. The original model and subsequent modifications predict that the average energy released as translational energy is a constant fraction of the available energy. It is pertinent to note that they predict the *average* internal energy in vibrations and rotations, but do not provide an adequate description of the *distribution* of internal energy, a knowledge of which is crucial to the analysis of our data. Although statistical distributions may be calculated, they tend to overestimate the amount of internal excitation. The amount of internal excitation is best obtained from measured kinetic energy distributions by invoking energy conservation

$$E_{vr} = E_{h\nu} - D_0^0(C_2F_4I\text{–}I) - E_{so}[I(^2P_{3/2})] - E_{trans}. \tag{8}$$

The photon energy is $E_{h\nu}$, the translational and internal energies are E_{trans} and E_{vr}, respectively. E_{so} is the electronic energy of I* referenced to that of I and D_0^0 is the bond dissociation energy. The average internal energy is obtained from Eq. (8) by simply using the average translation energy in the appropriate dissociation channel. The shape of the distribution is also essentially identical to that of the translation energy, with the energy scale shifted and reversed in direction, i.e., higher translation energy becomes lower internal energy.

The impulsive models predict 86% of the available energy appears as translation for a rigid radical and 14% for a soft one, the experimental value lying between these limits, which cover almost the full range of possibilities.[22] Experimental studies on a number of polyhaloethanes[6,7,9] show that approximately half of the available energy commonly appears as product translation energy. In particular, Reid *et al.* have measured the distribution of kinetic energy in the initial step of dissociation at 266 nm.[8] They found that the peak of the kinetic energy distribution was at 14 kcal/mol, which is 42% of the energy available at that wavelength. The distribution was fairly symmetric and broad, having a full-width at half-maximum (FWHM) value of 11 kcal/mol.

b. Estimation of rates

The unimolecular rates may be calculated as a function of the excess energy using statistical theories (e.g., RRKM),[23] provided the frequencies and rotational constants of the radical and its transition state are known. C_2F_4I is a very weakly bound molecule whose structure and vibrational frequencies are unknown. We avoid the pitfalls of estimating 16 vibrational frequencies for the parent and 15 for the transition state by choosing a different route for predicting $k_2(E)$. It has been found that in some cases the rates of unimolecular reactions in isolated molecules may be represented by an Arrhenius-like formula[24]

$$k_2(E) = A \exp\left[-\frac{\alpha}{E - E_0}\right]. \tag{9}$$

The pre-exponential factor A may be described as the effective frequency of the reaction coordinate. α is an adjustable parameter which may be interpreted as the product of the threshold energy E_0 and the number of effective oscillators. This imposes an upper bound of $\sim$120 kcal/mol. for the value of α.

The kinetic scheme used in this analysis is adequate for describing the dynamics provided the fitted values of the fast component are not taken at face value. The intrinsic assumption in any kinetic model is that the individual steps occur with a random distribution of lifetimes. This may not be an accurate description of direct mode reactions. In a recently described classical model,[25] the authors consider the rise time in terms of the relative velocity of separation and relate the distribution of fragment translational energies to the dis-

tribution of rise times for product states. Since the time resolution in these experiments cannot accurately determine the risetimes in the primary step, we do not consider these issues further. From a simple kinetics point of view, we note that Eq. (7) is a good approximation of Eq. (6) as long as $k_2 \leqslant 0.10k_1$. Since the initial dissociation is prompt, we have assumed that this condition holds for all rate constants considered.

c. Details of numerical simulations

In our first attempt at simulating the experimental transients, we calculated radical energy distributions with the following assumptions.

(i) We associated $I^{(1)}$ with I^* and $I^{(2)}$ with I. In other words, no I atoms are produced in the primary step.

(ii) The average energy in relative motion, and therefore the average internal energy in C_2F_4I, is a wavelength independent fraction of the available energy, as predicted by the impulsive models. This implies that the rigidity of the radical does not change with excitation energy. We used the measured fraction[8] of 42% in estimating the average translational energy at each wavelength.

(iii) The internal energy distribution is Gaussian, with width proportional to the average energy, i.e., the available energy. For consistency with experimental results, we used the values obtained in Ref. 8 to scale the width parameter.

(iv) The effects of angular momentum on the rates are not significant, i.e., we do not distinguish between rotational and vibrational energy in the radical. The estimated parameters describing the distributions, i.e., average energy and FWHM, used in these simulations are collected in Table I.

The rates of dissociation as a function of energy $k_2(E)$ were calculated for arbitrary choices of α and A using Eq. (9). The simulated time-dependent behavior, $S_e(t)$, of the ensemble of C_2F_4I for a given excitation wavelength and each pair of A and α was then obtained by calculating exponential rises weighted by the appropriate factors [Eq. (7)]. An experimental transient $D(t)$ was constructed as a two component exponential buildup using the lifetimes and relative amplitudes obtained from the nonlinear least squares fit of our data. $D(t)$ thus represents the deconvoluted molecular (ensemble) response underlying our experimental results. The effect of a finite instrument reponse on these simulations were accounted for by convoluting both the reference transient and the simulated transient with a typical response function. The convoluted transients, $\tilde{D}(t)$ and $\tilde{S}_e(t)$, were used to calculate a goodness-of-fit parameter, $\chi^2(\alpha,A)$, for each pair of α and A. χ^2 is defined as the weighted sum of squared deviations, normalized by the number of degrees of freedom

$$\chi^2(\alpha,A) = \frac{1}{N}\sum_{i=1}^{N} \frac{[\tilde{S}_e(t_i) - \tilde{D}(t_i)]^2}{\tilde{D}(t_i)}. \tag{10}$$

This function provides a one parameter representation of the quality of fit of the predictions of our model to the data and can be used to obtain a range of acceptable values for the two parameters A and α, given an appropriate cutoff.

Contour sections of $\chi^2(\alpha,A)$ for different excitation wavelengths (not shown) indicate that this model does not accurately describe the experimental results. The values of χ^2 are generally rather large, the overall minimum for each excitation wavelength being ~ 5 or greater. To compare the results of these simulations with our data more directly, we chose a pair of α and A values from the intersection of the χ^2 surfaces for the three longest excitation wavelengths and reconstructed $\tilde{S}_e(t)$ for each excitation wavelength. We then used a biexponential model to fit these transients in the same way that we analyzed the experimental ones. The parameters obtained from the fits of S_e and those derived from the data are listed in Table II. Representative $\tilde{S}_e(t)$ and $\tilde{D}(t)$ are shown in Fig. 6. The agreement between the lifetimes of the two components is fair, but the fraction of the shorter component predicted by the simulations is systematically larger than what we measured. The difference between simulations and experimental results, indicated more clearly by the null volume of intersection of the constructed error surfaces for small values of χ^2, leads us to reevaluate some of our assumptions in performing the above calculations.

3. Initial dissociation into the I channel

In Sec. III C 2 c, we assumed that initial dissociation into the I channel occurred with too low a probability for it

TABLE I. Parameters for simulations.

Excitation wavelength(nm)	E_{tot} (kcal/mol)	E^{26}_{avail} (kcal/mol)	$\langle E_{int} \rangle$ (kcal/mol)	FWHM[a] (kcal/mol)
266.0[b]	107.4	33.7	19.6	11
278.6	102.4	28.9	16.8	9.4
290.0	98.5	24.8	14.4	8.1
300.0	95.2	21.5	12.5	7.0
307.0	93.1	19.4	11.2	6.3
308.0	92.8	19.1	11.1	6.2
308.0[c]		19.1	6	5.2 (I^*)
		40.8	19	12.5 (I)

[a] Full-width at half-maximum of distribution.

[c] Measured parameters from Ref. 8.

[c] Measured parameters from Ref. 9. We have chosen distributions arising from a single channel of dissociation here. Thus the width corresponds to part of the measured distribution that has been attributed to initial dissociation into the I^* channel.

TABLE II. Lifetime analysis of experimental data and simulations.

Wavelength	Experimental			Simulation (A)		
(nm)	τ_1(ps)	τ_2(ps)	Fraction[a]	τ_1(ps)	τ_2(ps)	Fraction[a]
278.6	2	49	0.53	1.8	51.5	0.95
290.0	1	50	0.65	1.0	41	0.86
300.0	3	120	0.68	1.2	46	0.74
307.0	0.5	69	0.56	2.0	40	0.63

[a] Ratio of amplitude of fast component to total amplitude.
[b] The rate parameters for the simulations are $\alpha = 23$kcal/mol, and $A = 30.0\times 10^{12}\ s^{-1}$.

to affect our results, based on the results of Ref. 8 and the hypothesis that the surface crossing probability does not change significantly over the range of energies relevant to our experiments. This is supported by the IR fluorescence quantum yield measurements ($I^*\geqslant 0.9$) of Gerck at 308 nm.[18] On the other hand, it is sharply contradicted by the kinetic energy analysis of I atoms from the dissociation of $C_2F_4I_2$ at 308 nm[9], which indicates that $\sim 40\%$ of the initial dissociation leads to ground state I atoms. The quoted margins of error in the two experiments are not large enough to account for this substantial discrepancy. Clearly, a large fraction of I atoms formed during the initial step will affect the distribution of internal energy in the radicals and thereby have a non-negligible effect on our simulations, not to mention the contribution of the primary I atoms to the fast rise. We attempt to explore this possibility further by performing a new set of simulations which takes the quantum yield of I atoms in the first step into account.

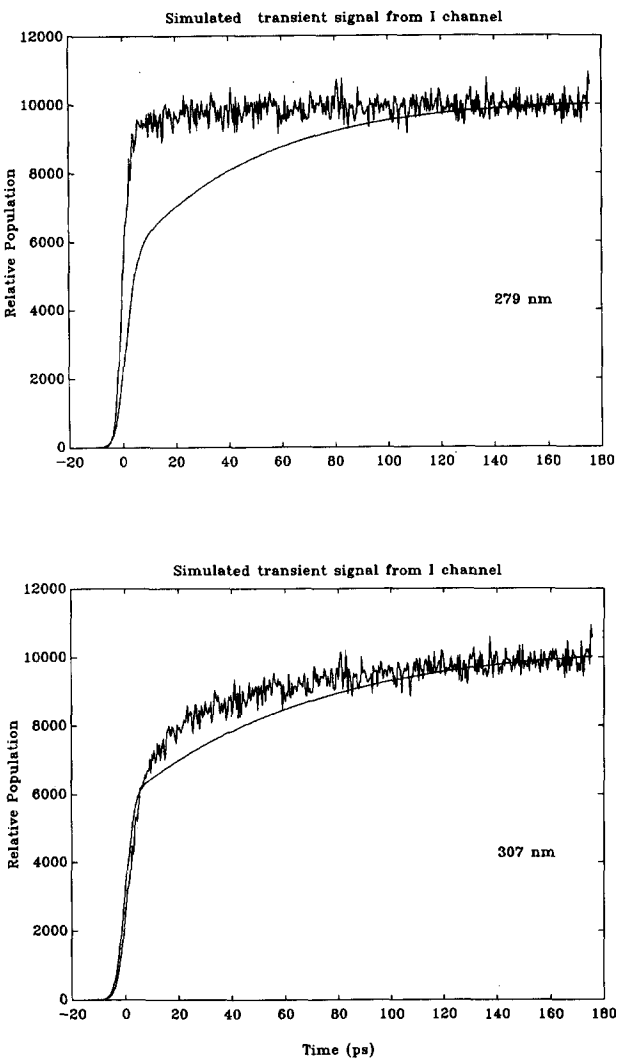

FIG. 6. Simulated ($\tilde{S}_e$) and reference ($\tilde{D}$) transients for two different excitation energies. $\alpha = 23$ kcal/mol and $A = 30\times 10^{12}\ s^{-1}$ were used for both transients. White noise (3%) has been added to $\tilde{S}_e$ to distinguish it from $\tilde{D}$ as well as to be more like the experimental transients. This also serves to reproduce any bias that the noisy data may impose on the ability of the curve-fitting algorithm to converge to final values.

The basic results from the study of Minton *et al.*[9] are that the distribution of kinetic energies is bimodal. One of the peaks (attributed to I* formation) appears at 13.1 kcal/mol and has a FWHM of ~ 5 kcal/mol, while the second one (due to I atoms) appears at 21.6 kcal/mol and has a FWHM ~ 12.5 kcal/mol. A number of conclusions may be drawn from a comparison of these results and those of Reid *et al.*[8] First, since dissociation at 266 nm leads to no significant amount of I atoms, their production must be wavelength dependent. Similar behavior has been observed in other alkyl halides and is surprising only to the extent that it also occurs in perfluorinated compounds, which generally tend to have high quantum yields of I*. Second, the average kinetic energy released into the I* channel on photolysis with 308 nm light is 69%, significantly higher than the observed 42% obtained on photolysis at 266 nm. Thus our assumption that the rigidity of the radical is independent of excitation energy is an oversimplification. Finally, the width of the distribution is narrower for dissociation at lower energies, proportional to the available energy, in concurrence with the *ad hoc* assumption made earlier.

Our experimental results are qualitatively consistent with an increasing quantum yield of I atoms at longer excitation wavelengths. Since the electronic energy (21.7 kcal/mol) is now available for internal motion, the radicals from this channel are formed with significantly higher internal energy and dissociate rapidly. In addition, the I atoms from the initial step will also be detected, leading to an expected transient shape given by the sum of Eqs. (4b) and (5), weighted by the relative quantum yields. A greater yield of I atoms at lower excitation energies would lead to a larger contribution to the signal from Eq. (4b) and, possibly, a larger relative fraction of the fast component.

The quantum yield of primary I atoms may be estimated

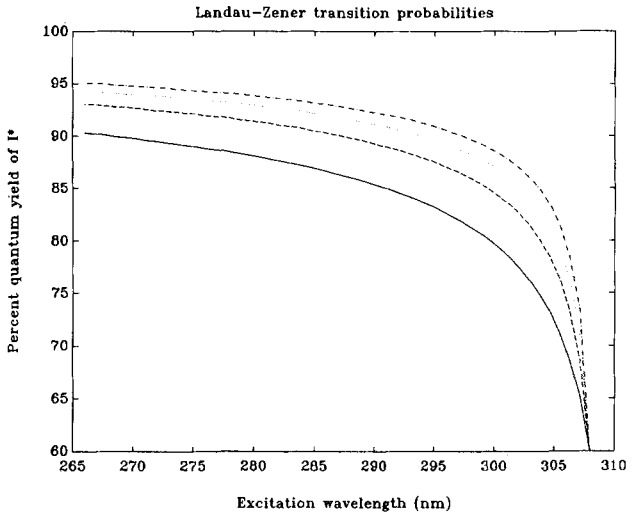

FIG. 7. Nonadiabatic transition probabilities calculated according to the Landau–Zener model. The curves actually show the probability that the system remains on the initial surface, thus representing the quantum yield of I* as a function of excitation energy, assuming a quantum yield of 0.6 at 308 nm and a range of values from 0.9 to 0.95 at 266 nm.

using the Landau–Zener (LZ)[27] theory for curve-crossing transition probabilities. In this theory, the probability ρ that the system remains on the initial surface depends on the kinetic energy E_{tr} of the reduced particle as given by Eq. (11)

$$\ln \rho \propto -\frac{1}{\sqrt{E_{tr}}}. \tag{11}$$

ρ as defined here corresponds to the yield in the I* channel. We use this relation to interpolate between the measured quantum yields of 0.6 and $\geqslant$0.9 at 308 and 266 nm, respectively, with the energy at which the curves intersect E_{cr}, as an adjustable parameter. The energy released is assumed to have been channeled into translational energy only, i.e., $E_{tr} = E_{avail} - E_{cr}$. The measurement at 266 nm reports a lower bound on the yield of I* based on the range of experimental error. Figure 7 shows the quantum yield calculated using this scheme for a number of values of ρ at 266 nm, all chosen larger than the bound imposed in Ref. 8. The values of E_{cr} obtained in the fitting procedure are quite large, varying from 18.5 to 19.0 kcal/mol depending on our choice of ρ at 266 nm. Considering that the total available energy at 308 nm is 19.1 kcal/mol, we conclude that in this simple picture, excitation at 308 nm corresponds to excitation very close to the crossing point.[28]

Simulations for this revised model were done in much the same way as described in Sec. III C 2 c using convolutions for the relevant transients. The two variations were (1) we used two Gaussian curves with independently chosen peak positions and widths to simulate the internal energy distributon in the radicals, and (2) we used the LZ scheme illustrated in Fig. 7 with I* yield of 0.95 at 266 nm to predict the yield at intermediate energies. The parameters used are listed in Table III.

The overall agreement between this model and our data is better, as evidenced by the fact that the individual minima

TABLE III. Parameters for simulations assuming both channels open in primary step.

Excitation	I* channel		I channel	
wavelength (nm)	$\langle E_{int} \rangle$[a]	FWHM[b]	$\langle E_{int} \rangle$[a]	FWHM[b]
278.6	15.1	9.4	23.5	15.2
290.0	11.3	8.1	21.6	14.0
300.0	8.2	7.0	20.0	13.0
307.0	6.3	6.0	19.1	12.5
308.0[c]	6.0	5.2	19.0	12.5

[a] Energy units are kcal/mol.
[b] Full-width at half-maximum of distribution.
[c] Measured parameters from Ref. 9. We have chosen Gaussian distributions for our simulations, although Ref. 9 does not make such a claim.

are lower (minimum $\chi^2 \sim 3$). This suggests that there is indeed a small fraction of I atoms formed in the primary step. However, as in the previous simulations, we cannot identify a significant region of (α,A) space, where the error between the predictions of the model and the data is uniformly small. The bimodal energy distribution has a rather large effect on the simulations for the redder excitation wavelengths due to the fact that E_0, the threshold energy for decomposition, is comparable to the median energy in the nascent radical. If E_0 were lower[29] than the value of 8.1 kcal/mol we used throughout our calculations, the error surfaces generated for the lower photolysis energies would be significantly affected, but the overall agreement between model and experimental results is not likely to improve.

4. Evaluation of the results from simulations

The discussion of the last two sections points to the importance of the distribution of internal energy in explaining the observed inhomogeneous buildup of products from a reactive ensemble. The LZ approximation suggests that the dispersion of lifetimes is dominated by the distribution of internal energies resulting from the I* channel, particularly at the bluer excitation wavelengths.

In the case of a perfect agreement between model and data, we would be able to identify a small range of values for the parameters A and α which simultaneously minimize the error at all excitation wavelengths. The fact that our model does not produce such a well-defined set of values leads one to question its quantitative accuracy. It is therefore pertinent to reiterate some of the approximations we have made in developing this model and present our appraisal of their significance to the discrepancy between model and data. First, we assumed Gaussian distributions and a simple *ad hoc* scaling (interpolation) scheme for the average energy and width. In the absence of experimental data at *all* relevant energies, such a scheme appears reasonable. Since our estimates of the average energy are based on measured distributions, we expect them to be close to their correct values. The choice of a Gaussian shape for the distributions is likely to have a minor impact on our calculations, particularly considering the widths of these distributions. However, if the

correct shapes were strongly asymmetric, and had tails of significant amplitudes on either or both edges, the effect could be quite large. Second, we have used Eq. (7) instead of Eq. (6) which is the proper choice for the kinetic model. We consider this to be of minor significance also, especially because the very fast decomposition rates where this approximation may fail are much faster than the response function and the effects would be averaged out. Third, we have neglected the possible role of angular momentum in determining the rate of radical decomposition. While this is a limitation in our model, we note that any attempt to include the effects of angular momentum would involve additional approximations and assumptions. We leave such considerations for future refinements of the model.

Fourth, the prescription for $k_2(E)$ [Eq. (9)] used in all of the simulations presented here may not be strictly valid over the full range of relevant energies. It is interesting to note that applications of more detailed theories of bond-fission rates have failed in quantitatively predicting rates near threshold.[1,30] While the experimental results presented here do not provide direct measurements of microcanonical rates for this system, we may deduce an approximate $k_2(E)$ from the simulations. In Fig. 8, we show plots of k_2 using values of A and α corresponding to the minimum of the error surface for each excitation wavelength. The corresponding Gaussian distributions (Table I) are shown in the lower panel. Using these curves, we construct an average function $k_d(E)$, which is perhaps more representative of the correct energy dependence of the rate of radical decomposition. This curve is shown as a heavy solid line. Transients calculated using $k_d(E)$ should show a uniform similarity to the experimental transients over all excitation energies. Clearly, the accuracy of this function depends on how precisely we were able to estimate the internal energy distribution at each wavelength.

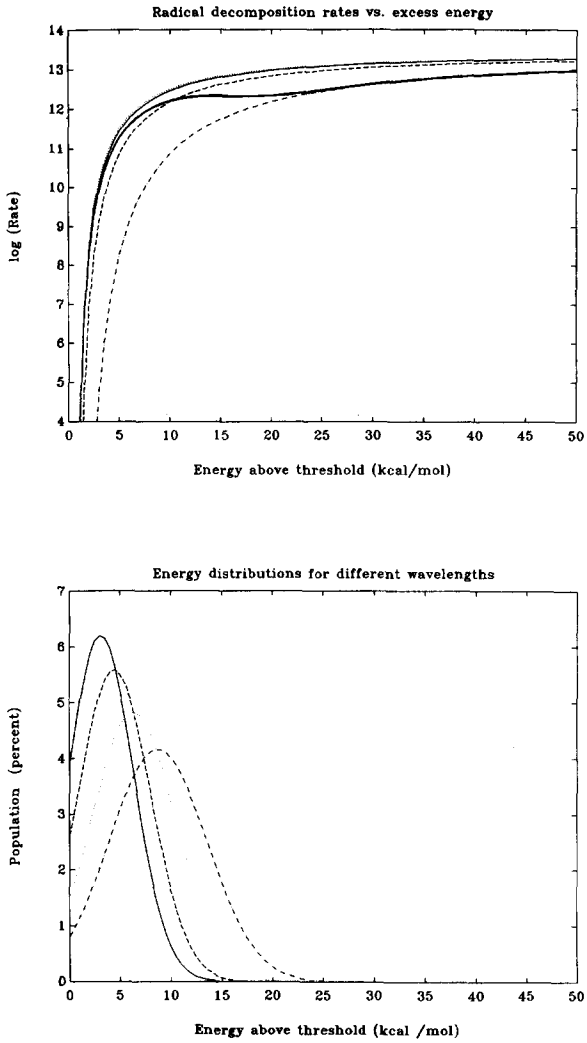

FIG. 8. Rates as a function of energy. The different curves correspond to (α,A) values at the minimum of each error surface calculated using the parameters in Table I and including convolution. The thin solid line corresponds to 307 nm, the dashed line to 300 nm, the dotted line to 290 nm and the dot–dashed line to 278.6 nm. The assumed energy distribution for the four different cases are displayed in the lower panel, using the same line types. The heavy solid line signifies an empirical average rate $k_d(E)$.

IV. CONCLUSIONS

In this paper, we have presented picosecond studies of the dynamics of consecutive bond breaking in the dissociation reaction of $C_2F_4I_2$. Reaction rates as a function of excitation energy are deduced. The dynamics of this reaction can be described in terms of a two step mechansim, the first one leading to an internally excited radical, C_2F_4I, in less than 1 ps, the second step being the dissociation of these energized radicals (average lifetime $\sim$30–150 ps depending on total energy). The buildup of ground state I atoms appears biexponential, partly because radicals formed with different amounts of internal energy dissociate with different rate constants. We find that a threshold energy of $\leqslant$8 kcal/mol, as measured in a recent molecular beam experiment,[9,29] is in fair agreement with our observations. Our results support the hypothesis that the initial dissociation can produce both I and I* atoms, their relative quantum yields being a function of the excitation energy.

ACKNOWLEDGMENTS

This research was supported by the National Science Foundation. We wish to thank Dr. J. L. Knee, Dr. B. Reid, Professor R. Bersohn, and Professor Y. T. Lee for many stimulating discussions. We also thank A. J. Hoffman for help with the experiments and N. Kurur and Dr. J. Yesinowski (C.I.T.) for their assistance in obtaining the ^{19}FNMR spectrum of our sample. Finally, we would like to express our sincere thanks to the referee for a critical reading of the manuscript and many helpful comments.

[1] L. R. Khundkar, J. L. Knee, and A. H. Zewail, J. Chem. Phys. **87**, 77 (1987); N. F. Scherer and A. H. Zewail, *ibid.* **87**, 97 (1987); J. L. Knee, L. R. Khundkar, and A. H. Zewail, *ibid.* **87**, 115 (1987); E. Potter, M. Gruebele, L. Khundkar, and A. Zewail, Chem. Phys. Lett. **164**, 463 (1989).
[2] J. L. Knee, L. R. Khundkar, and A. H. Zewail, J. Chem. Phys. **83**, 1996 (1985).
[3] See, for example, R. D. Levine and R. B. Berstein in *Molecular Reaction Dynamics and Chemical Reactivity* (Oxford University, New York, 1987).
[4] M. Dzvonik, S. Yang, and R. Bersohn, J. Chem. Phys. **61**, 4408 (1974); J. H. Ling and K. R. Wilson, *ibid.* **65**, 881 (1976); R. N. Zare, Mol. Photo-Chem. **4**, 1 (1972); S. R. Gandhi, T. G. Curtis, and R. B. Bernstein, Phys. Rev. Lett. **59**, 2951 (1987).
[5] See, for example, S. R. Leone, Adv. Chem. Phys. **44**, 255 (1982); S. J.

Riley and K. R. Wilson, Faraday Discuss. Chem. Soc. **53**, 132 (1972); R. Bersohn, J. Phys. Chem. **88**, 5145 (1984); R. F. Frey, J. O. Jensen and J. P. Simons, *ibid.* **89**, 788 (1985).

[6]D. Krajnovich, L. J. Butler, and Y. T. Lee, J. Chem. Phys. **81**, 3031 (1984); T. K. Minton, G. N. Nathanson, and Y. T. Lee, *ibid.* **86**, 1991 (1987).

[7]L. J. Butler, E. J. Hintsa, S. F. Shane, and Y. T. Lee, J. Chem. Phys. **86**, 2051 (1987).

[8]Brian Reid, Ph.D. thesis, California Institute of Technology, 1986.

[9]Timothy K. Minton, Ph.D. thesis, Univ. of California, Berkeley, 1986.

[10]G. E. Busch and K. R. Wilson, J. Chem. Phys. **56**, 3626, 3638 (1972).

[11]N. F. Scherer, Ph.D. thesis, C.I.T., 1989.

[12]V. Wray, Ann. Rep. NMR Spectrosc. **14**, 1 (1983).

[13]J. J. Tiee, M. J. Ferris, G. W. Loge, and F. B. Wampler, Chem. Phys. Lett. **96**, 422 (1983).

[14]W. H. Press, B. P. Flannery, S. A. Teukolsky, and W. T. Vetterling *Numerical Recipes* (Cambridge University, Cambridge, 1986); D. W. Marquardt, SIAM, **11**, 431 (1964).

[15]R. S. Mulliken, Phys. Rev. **51**, 310 (1937); R. S. Mulliken, J. Chem. Phys. **8**, 382 (1940).

[16]C. A. Wright and S. R. Leone, J. Phys. Chem. **87**, 5299 (1983); H. B. Schlegel and C. Sosa, *ibid.* **88**, 1141 (1984); T. Donahue and J. R. Wiesenfeld, J. Chem. Phys. **63**, 3130 (1975).

[17]M. Kawasaki, S. J. Lee, and R. Bersohn, J. Chem. Phys. **63**, 809 (1975).

[18]E. Gerck, J. Chem. Phys. **79**, 311 (1983).

[19]P. M. Kroger, P. C. Demou, and S. J. Riley, J. Chem. Phys. **65**, 1823 (1976).

[20]The observed resonant enhancement via a two-photon state of neutral I atoms implies that our experiment probes the dynamics of some dissociation channel where neutral iodine atoms are produced. Pathways that lead directly to I^+ ions would be manifested in the background signal since the signal from such a channel does not depend on the time delay between pump and probe pulses. A similar point has been discussed in some detail previously (Ref. 1, Knee *et al.*).

[21]A. J. Tuck, Faraday Discuss. Chem. Soc. **62**, 689 (1976).

[22]In passing, it may be noted that a united atom model using the mass of CF_2 instead of the bare C atom predicts 44% of the available energy should appear as translation, a value which is much closer to the observed value. This approach corresponds to having the C–F bonds of the α carbon atom being rigid, while the rest of the radical is flexible.

[23]See, for example, P. J. Robinson and K. A. Holbrook, *Unimolecular Reactions* (Wiley-Interscience, London, 1974).

[24]A. H. Zewail, Faraday Discuss. Chem. Soc. **75**, 315 (1983).

[25]R. Bersohn and A. H. Zewail, Ber. Bunseges. Phys. Chem. **92**, 373 (1988).

[26]The threshold for dissociation of C_2F_4I was calculated using the following thermochemical parameters. Heats of formation at 0 K: $C_2F_4I_2$ (-165.4 kcal/mol), I (25.63 kcal/mol), C_2F_4 (-156.6 kcal/mol). D_0^0 (CF_2ICF_2–I) = 52.0 kcal/mol. These values were all obtained from Ref. 9.

[27]See, for example, E. E. Nikitin and S. Y. Umanskii, in *Theory of Slow Atomic Collisions* (Springer, Berlin, 1984), p. 273.

[28]It may be worth recalling our earlier comment on how excitonic interactions may possibly affect the energy at which the states cross.

[29]G. N. Nathanson, T. K. Minton, S. F. Shane, and Y. T. Lee, J. Chem. Phys. **90**, 6157 (1989).

[30]S. J. Klippenstein, L. R. Khundkar, A. H. Zewail, and R. A. Marcus, J. Chem. Phys. **89**, 4761 (1988).